HYDROACOUSTIC T PHASES FROM LARGE ICEBERGS DRIFTING IN THE ROSS SEA

Emile A. Okal[1], Jacques Talandier[2], and Olivier Hyvernaud[2]

Northwestern University[1]; Laboratoire de Géophysique, Papeete, Tahiti[2]

Sponsored by Defense Threat Reduction Agency[1] and Commissariat à l'Energie Atomique[2]

[1]Contract Number DTRA01-00-C-0065

ABSTRACT

In Late 2000, numerous sequences of T phases were detected by seismic stations of the Polynesian network and in the Cook Islands, with an origin in the Ross Sea off the coast of Antarctica. This observation was corroborated by records at seismic stations, at permanent sites VNDA and SBA, and at the volcano monitoring network on Erebus. A combined location procedure using both seismic phases (presumed to be Lg) and T phases, narrowed down the source of the activity to huge icebergs which at the time were drifting in the Ross Sea after calving off the Ross Ice shelf. The signals present a broad variety of spectral characteristics, most of them featuring prominent eigenfrequencies in the 4-to-7 Hz range, often complemented by overtones. Most epicenters follow the spatio-temporal evolution of the drift of iceberg B15-B. The majority of the signals are generated during a 36-day time window when it is speculated that B15-B collided with smaller icebergs or was scraping the ocean floor on the shallow continental shelf. We speculate on the possible physical nature of the resonator generating the signals, which could correspond to an elastic mode of the iceberg, or to the oscillation of the fluid-filled crack in the ice. The signals differ from those previously recorded during volcanoseismic swarms in that the spectral lines have a much higher quality factor Q (in general found to be > 100). Such oscillations document a new source of acoustic energy in the ocean column, which is of general interest in the framework of the CTBT. The location procedure used in this context also underlines the powerful synergy which can be developed between various kinds of geophysical data. In 2002, more such signals are being recorded from various sites aound Antarctica, and we also report on these developments, following the break-up of a gigantic segment of the Ross Ice shelf on 2002 May 10.

OBJECTIVE

The objective of this research is the analysis of the source characteristics of hydroacoustics signals in the world's oceans, and in particular the discrimination between man-made explosions and natural sources, such as earthquakes, landslides and volcanoes. We report here on the identification of a new source capable of contributing significant hydroacoustic energy over extended periods of time.

RESEARCH ACCOMPLISHED

Starting in August 2000, seismic stations operating as T –phase stations in Polynesia detected irregular activity originating from the Southern Ocean. The activity was concentrated in a group of 13 sequences (hereafter the "Ross Events") whose principal characteristics are listed in Table 1, with representative spectrograms of signals shown on Figures 1a-d. At seismic stations located on atolls, such as Vaihoa (VAH), the acoustic-to-seismic conversion is particularly efficient, and the seismic signal at the T –phase station can be regarded as essentially equivalent to the acoustic one inside the SOFAR, within the frequency window of interest ($2 \leq f \leq 16$ Hz). In most instances, the energy of the Ross events is concentrated at one or several prominent frequencies, which suggests that its source must involve the oscillation of some kind of resonator, a model also supported by the often long duration of the signals, e.g., Event 4, which lasts for 3 hours. However, some sequences feature significantly broader spectra (e.g., Event 12), and some like Event 2 (Figure 1a) last no more than 2 minutes. In addition, the frequency of the largely monochromatic signals does fluctuate with time, a property already observed during the Hollister volcanic swarm (Talandier and Okal, 1996), with some of the Ross events featuring more substantial variations of frequency with time (e.g., Event 7), which give the spectrograms a contorted, "snake-shaped" aspect. Finally, several sequences end with singular signals exhibiting an increase of frequency with time (suggestive of the shrinking of the resonator), which can be slow and gradual (Event 4) or fast and abrupt (Event 3, Figure 1b). In the case of Event 13, the termination of the sequence involves a complex evolution of prominent frequencies with time, featuring several episodes of frequency decrease, a property termed "gliding" and identified during episodes of volcanic tremor (Hagerty et al., 1997) which in general terms would suggest a geometrical expansion of the resonator (Chouet, 1996).

A systematic effort was conducted to complement the Polynesian dataset with records at other Pacific seismic stations. When available, the IRIS station at Rarotonga (RAR) provided increased azimuthal aperture; the station was, however, inoperative from 04 to 18 December 2000. Unfortunately, no other seismic station could contribute T –phase signals, and this for a variety of reasons, including blockage at NOUC, JOHN, and at the ocean-bottom observatory H2O; unfavorable station locations involving long post-conversion seismic paths (TAU, KIP, XMAS); a probable combination of those two effects at VIB; and a high level of background noise at the small island of Pitcairn (PTCN). Finally, no signal was detected at Easter Island (RPN), where detection of T phases has been previously recognized as irregular (Okal and Talandier, 1997; Okal et al., 2001; Reymond et al., 2001).

The principal events in the sequence were first located using the techniques developed by Talandier and Okal (1996) during the Hollister volcanic swarm: using whenever possible impulsive arrival times of sharp sub-events, or in their absence, differential travel-times between stations by cross-correlating the fluctuations with time of the frequency of quasi-monochromatic T waves. After implementing station corrections to compensate for the post-conversion land path, the locations of the sources were inverted using the seasonally adjusted, laterally varying model of acoustic velocities of Levitus et al. (1994). The location procedure is enhanced by a Monte Carlo algorithm consisting of injecting Gaussian noise into the dataset of arrival times (Wysession et al., 1991); a best-fitting ellipse is then computed for the resulting cluster of epicenters.

In all cases, these preliminary epicenters locate in the general area of the Ross Sea, and of the Borchgrevink and George V coasts of Antarctica, but the limited azimuthal coverage provided by the band of available stations (at most 30°) results in weak resolution of epicentral distance. Nevertheless, several statistically distinct groups can be identified, with Events 2 and 13 along the coasts, while the remaining epicenters locate in the center of the Ross Sea.

In view of these preliminary results, we conducted a systematic search for additional records of conventional seismic waves at Antarctic stations. We were able to identify signals at the IRIS station at Scott Base (SBA), at the GTSN station Vanda (VNDA), and at several stations of the Mount Erebus Volcanic Observatory (MEVO), located on Ross Island (courtesy of Dr. Richard Aster).

In order to use the Antarctic seismic signals in a combined relocation with the Polynesian T phases, we need to know the velocity of seismic waves along the source-to-receiver path. For this purpose, we tested a series of relocations, for variable values of the velocity V to the Antarctic stations. In this experiment, we used a priori bounds of $V_{\min} = 1.3$ km/s, thus including the possibility of an acoustic velocity in the cold waters of the Southern sea, and $V_{\max} = 8.25$ km/s, corresponding to a P_n velocity under the continental shelf, and we varied V in increments of 0.05 km/s. For each value of V, we quantify the quality of the relocation through the root-means squares of the residuals, σ. We determined that the best-fitting value of V is consistently $V_{opt} = 3.7 \pm 0.2$ km/s.

The interpretation of V_{opt} is not straightforward, and remains somewhat unresolved. On the one hand, it matches well the velocity of P waves in recrystallized ice (Thiel, 1961). However, and even in the case of Event 1, which may have occurred on the Ross Ice Shelf or at its boundary (see below), this interpretation is improbable, since the ice shelf is only 300 m thick, i.e., less than 1/5 of the longest wavelengths recorded in Antarctica. For the other events located farther North, satellite imagery disproves the existence of a continuous layer of thick ice along the path to VNDA.

Rather, we propose to interpret the arrivals at $V_{opt} = 3.7$ km/s as L_g wavetrains, and interpreted as shear energy trapped in the continental crust (e.g., Knopoff, 1973). As documented, for example by Bouchon (1982) and Campillo et al. (1984), L_g can be the first prominent arrival at regional distances in conditions where P arrivals do not emerge from noise, in particular for shallow crustal dislocation sources. In addition, L_g energy can propagate efficiently at frequencies of a few Hz (Bouchon, 1982). Furthermore, the value of V_{opt} falls in the range of predicted and observed L_g velocities in the relevant frequency window (Cara and Minster, 1981). Finally, we will see that the epicentral locations of the Ross Sea events are on the continental shelf or at its boundaries, so that L_g wavetrains would not be blocked by transit over an oceanic path.

Notwithstanding our inability to definitely identify the nature of the seismic phases recorded at Antarctic stations, we will use the optimized velocity $V_{opt} = 3.7$ km/s for all seismic phases at Antarctic stations in order to locate the Ross events from a combined dataset of acoustic and seismic arrival times.

As discussed in Table 1, out of the 13 sequences investigated, we obtain seven very well constrained locations, with semi-major axes of ≈ 25 km for the Monte Carlo ellipses (Events 2, 3, 5, 8, 10, 11, 12), and two poorly resolved ones (Events 1 and 13). The remaining sequences (Events 4, 6, 7, 9) are given tentative locations based on their temporal association with well-located events. As shown on Figure 2, all epicenters, except Events 1, 2, and 13, fall in the center of the Ross Sea. The location of Event 13 (Figure 1d), which was recorded neither by the Antarctic stations nor by RKT, could not be improved beyond the estimate obtained from Polynesian T phases. Event 1 (15 August 2000) has a large uncertainty, but lies significantly South of the November-December group. As for Event 2 (08 November 2000), it has a well constrained epicenter just South of Cape Adare on the Borchgrevink Coast.

We reject volcanism as a possible origin of the Ross Sea events. First, an important aspect of our results is that all nine located events cannot share a common epicenter. This is well documented by the Monte Carlo ellipses on Figure 2, and was confirmed by a formal attempt at inverting the full dataset of arrival times for a common epicenter and distinct origin times, which resulted in unacceptable residuals of more than one minute. We conclude that the location of the Ross Sea events moved with time in a generally SE to NW direction (with the exception of Event 2). Their spatio-temporal evolution is in sharp contrast with our previous experience of long-range hydroacoustic detection at volcanic sites such as Macdonald Seamount and Hollister Ridge (Talandier and Okal, 1996). Second, we note the presence of three known sites of volcanic (or fumarolic) activity in the area: Erebus (77.6°S; 167.2°E), Melbourne (74.35°S; 164.70°E) and the Balleny Islands (66°S; 163°E). When tested as possible epicenters for our datasets, r.m.s. residuals exceeding several minutes made all of these locations unacceptable. In the case of Event 12, for example, Erebus was a legitimate epicenter on the basis of the RSP hydroacoustic data alone). However, the inclusion of the Antarctic dataset leads to a discrepancy of more than 9 minutes between Polynesian and Antarctic stations. We reject volcanism as a source of the Ross Sea events, since even an uncharted volcanic source would have had to move hundreds of km across the Ross Sea over a period of a few weeks.

Rather, we propose that the sources of the Ross Sea events lie within very large icebergs, documented to have calved off the Ross Ice Shelf in the [Northern] Spring of 2000, and which were drifting across the Ross Sea in a northwesterly direction during the later part of the year. We base our interpretation on the dataset of reported coordinates and infrared satellite photographs available from the web site of the University of Wisconsin's Antarctic Meteorological Research Center (Anonymous, 2002a).

Around March-April 2000, Iceberg B-15 (300 km by 40 km) and the smaller B-17 to the East calved off the shelf around 78°S, between 177 and 165°W. By 15 August 2000, the date of Event 1, B-15 had broken up into two principal pieces, B-15A and B-15B, and several smaller fragments. B-15B then takes a Northerly path towards the Center of the Ross Sea, at an average drift velocity of 4 km/day (or 5 cm/s). Figure 2 plots the positions of B-15B and B-17 at a number of dates between 09 November 2000 and 05 January 2001. During that time window, B-15B engages in a large rotation, collides with B-17 in Early November 2000, calves off a further small fragment, B-15F, on its West side, some time between 14 November and 29 November 2000, and frees itself from B-17 as the latter breaks into pieces around 30 December 2000. By 05 January 2001, B15-B has taken a Northwesterly direction, rounds Cape Adare about 03 May 2001 (it has then broken into two parts), and then progresses along the Oates Coast, where it currently (2002) lies around 155°E (Anonymous, 2002b).

As documented on Figure 2, there is a spectacular correlation between the epicenters of Events 3, 5, 8, 10, 11 and 12 (and hence presumably of the intervening Events 4, 6, 7, 9) and the location of the icebergs B15-B and B-17. In particular, the spatio-temporal evolution from the Southeastern group of epicenters (3, 5, 8) in November to the Northwestern one (10, 11, 12) in December mimics the drift and rotation of B-15B. In the case of the relatively poorly located Event 1 (on 15 August 2000), Figure 2 shows the Northern end of the large Monte Carlo ellipse similarly intersecting the position of B15-B on that same day.

On this basis, we propose that the source of the Ross Sea events consists of unidentified phenomena taking place inside large icebergs (principally B15-B) drifting in the Ross Sea.

As discussed below, we can offer only vague speculation as to the nature of the events taking place inside the icebergs and generating the hydroacoustic and seismic signals studied. Whatever these phenomena may be, it is remarkable that they take place only during a small part of the long drift of B-15B from the Ross Ice shelf to Cape Adare and beyond, namely during a 36-day window and over a distance of less than 200 km (with the exception of Event 1, farther South). In particular, B-15B becomes silent after 18 December 2000, and during its 4-month voyage to Cape Adare. We know of no prominent bathymetric feature which would explain this pattern through hydroacoustic blockage along the path to Polynesia. Rather, B-15B's silence must reflect the cessation of the physical source process.

Among possible mechanisms for the excitation of an oscillator, that would be geographically (or temporally) controlled, we envision collisions with other ice masses, and rubbing on the sea floor. A possible scenario would correlate the Ross Sea events with the collision between B-15B and B-17, which lasted at least one month, until B-17 breaks into pieces at the end of December. Another scenario would be to invoke friction on the floor of the Ross Sea. Bathymetric coverage of the Ross Sea is scarce, especially since the relevant area lies outside the Southern limit (72°S) of Smith and Sandwell's (1994) satellite altimetry database. However, the Northern portion of B-15B's path (traveled Westwards after 01 January 2001) most probably lies over deep water, whereas its Southern portion (traveled Northwards) is over the continental shelf. We can only speculate as to the presence of large seamounts or other underwater structures, against which the iceberg could have rubbed, but the spatio-temporal distribution of the Ross Sea events would be in very general agreement with this scenario. We also note that significant iceberg furrows have been documented on the sea floor, including around Antarctica, at depths as great as 400 to 500 m (Harris and Jollymore, 1974; Barnes and Lien, 1988), making it legitimate to assume that motion over the continental shelf at similar depths would occasionally involve scraping against bathymetric features. Finally, as shown by Campillo et al. (1984), a superficial source (such as an iceberg scraping the ocean floor) will excite L_g most efficiently, whereas the excitation of P_g would be relatively insensitive to depth; these properties would lead naturally to L_g being the prominent seismic phase for sources exciting the solid Earth at the water-crust interface.

Regarding the actual physical nature of the sources generating the Ross Sea signals, the prominence of distinctive frequencies (typically 4 Hz) in many spectra (occasionally with harmonics) suggests the oscillation of a resonator. In this respect, our sources differ significantly from the "icequakes" widely observed ever since seismic stations were installed on glaciers and large icecaps. Being essentially instantaneous sources, the latter are characterized by short durations and a broad spectrum featuring high frequencies (Sinadinovski et al., 1999). Even the so-called "low-frequency icequakes" attributed to calving of ice blocks from glaciers (Qamar, 1988) and occasionally featuring a monochromatic spectrum (VanWormer and Berg, 1973) are of much shorter duration than the Ross events.

In order to investigate more in detail the spectral characteristics (eigenfrequency and quality factor *Q*) of a representative signal, we selected the VAH record from Event 4 (on 12 November 2000) because of its exceptional duration (3 hours). For this purpose, we use a running window of 81.9 s duration (4096 samples), offset 10 s at a time. At

each step, we then identify the frequency f_0 at which the spectral amplitude $X(f)$ reaches its maximum, which we interpret as the eigenfrequency of the resonator, and we fit a resonance curve of the form

$$X_r(f) = \frac{A}{\sqrt{(f - f_0)^2 + \frac{\pi^2 f_0^2}{Q^2}}} \tag{1}$$

to the shape of the spectral amplitude $X(f)$ in the frequency interval $I\ \{f_0 - 0.125\,\text{Hz} \le f \le f_0 + 0.125\,\text{Hz}\}$. We retain only values of Q for those windows where $X(f_0)$ is at least 40% of its maximum value, and for which the spectral line is adequately modeled by (1), as defined its goodness of fit. The two frames on Figure 3 show the variation of f_0 and Q as a function of time t, taken at the center of the running window.

While f_0 can remain remarkably constant over intervals of time of a few minutes (see Figure 1), Figure 3a shows that it varies significantly on a time scale of tens of minutes. Changes in f_0 can be continuous (e.g., the "gliding" observed at the start of the record), or sharp and stepwise, the windows with stronger and cleaner signals being more stable in frequency. This would require the presence of several oscillators, some of which capable of an evolution with time of their eigenfrequency, which in turn most probably expresses an evolution of their dimension.

The quality factors Q of the resonators range between 100 and 650, with an inverse average value of 250, much greater than typically reported for volcanic tremor (Q = 5 to 10) or even during the Hollister swarms (Q = 20 to 50); this further argues strongly against a volcanic origin for the Ross Sea signals. The attenuation of seismic waves in ice has been reported in the Greenland icefield by Langleben (1969) who reported a fall-off coefficient $c_1 = 4.45 \times 10^{-2}$ dB m^{-1} kHz^{-1} equivalent to Q = 166, and in sea ice by Kohnen (1970), who gives a slope of attenuation with frequency $q = 0.56 \times 10^{-5}$ m^{-1} Hz^{-1}, equivalent to Q = 175. Note however that these values were measured at considerably higher frequencies in both studies, and on longitudinal waves in the latter.

Speculating further on the possible physical nature of the resonator, we note the approximate dimensions of B-15B, 135 km by 40 km, and we take its thickness as at least 300 m, based on an estimation of the emerged fraction from airborne photographs, and of the thickness of the Ross Ice shelf from seismic soundings. We can then eliminate gravitational oscillations as the source of the signals, since the bobbing frequency of the iceberg on the sea would be on the order of 30 mHz, rather than 4 Hz. Rolling and pitching eigenfrequencies would also be much lower than observed — on the order of 20 mHz.

Rather, the frequencies observed could represent various eigenmodes of oscillation of the iceberg. For example, for a 300-m thick ice layer, the eigenfrequency of a vertical shear mode would be 3.07 Hz (with $\beta = 1.84$ km/s, or a Poisson ratio of 0.34). The eigenfrequency of a fundamental "Crary" mode (Ewing and Crary, 1934; essentially a shear wave propagating horizontally with a phase velocity equal to the P –velocity α) would be 3.51 Hz for the ice sheet in a vacuum; it could be affected by the presence of water (Press and Ewing, 1951), but its order of magnitude would remain in general agreement with the resonance frequencies observed in our signals. This interpretation would be particularly likely under the assumption that the ice mass is set in resonance by scraping the ocean floor, or rubbing against another ice mass; it could also explain the presence of harmonics, or overtones, since several modes would be excited by a source essentially similar to hitting a bell, and resulting in musical "richness". However, under this scenario, the iceberg would be expected to resonate at a set of discrete, and well defined pitches, and the observed continuous fluctuation of eigenfrequency with time would be more difficult to explain.

Another scenario would involve the resonance of a fluid-filled cavity in a mode comparable to the oscillation of magma within a fissure in a volcanic system (Aki et al., 1977). As summarized by Chouet (1996), the eigenfrequencies of such as a resonator are complex functions of its size and shape, and of the impedance contrast between the fluid filling the crack and the surrounding medium. In the particular case of icebergs, the fluid would have to be water, but the almost certain presence of air bubbles could greatly reduce the sound speed in the fluid. Furthermore, this model could explain the observed fluctuations of frequency with time, as both the dimension of the resonator and the supply of air bubbles could be expected to vary with time continuously, for example during filling or emptying of the fluid in the crack. These interpretations remain of course highly speculative at this point.

CONCLUSIONS AND RECOMMENDATIONS

We have documented prolonged episodes of hydroacoustic activity in the Ross Sea during the months of August-December 2000. By combining datasets of T phases recorded in Polynesia with regional seismic phases recorded at

Antarctic stations, we obtain epicentral locations correlating systematically with the position of large icebergs, specifically B-15 B and B-17, which were drifting in the Ross Sea at that time, and thus we conclude that the signals originated at or inside the icebergs. This study illustrates the powerful synergy obtained by combining hydroacoustic and classical seismological datasets, and resulting in epicentral precision of a few tens of km in a very remote area of the world's oceans.

Despite a broad variability in the spectral characteristics of the Ross events, they cannot be compared to seismic sources previously identified and analyzed in the ice environment, such as icequakes and calving events. Rather, our observations define a new kind of source capable of contributing hydroacoustic energy to the SOFAR channel over extended periods of time. The presence of preferential frequencies in the 3 to 7 Hz range (often associated with overtones) clearly implicates the resonance of an oscillator, whose exact nature presently eludes us. In the context of the use of hydroacoustic waves for explosion monitoring, it is clear that a deeper investigation of the phenomena involved is warranted; a possible avenue would involve the direct deployment of portable seismic stations on massive icebergs known to be calving off the major Antarctic ice shelves (May 2002).

REFERENCES

Aki, K., M. Fehler, and S. Das (1977), Source mechanism of volcanic tremor; fluid-driven crack models and their application to the 1963 Kilauea eruption, *J. Volcanol. Geotherm. Res.*, 2, 259−287.

Anonymous (2002a), Antarctic Meteorological Research Center, http://amrc.ssec.wisc.edu, Univ. Wisconsin, Madison.

Anonymous (2002b), National Ocean and Atmospheric Administration, http://www.noaanews.noaa.gov/ stories/s862.htm, U.S. Dept. of Commerce.

Barnes, P.W., and R. Lien (1988), Icebergs rework shelf sediments to 500 m off Antarctica, *Geology*, 16, 1130−1133.

Bouchon, M. (1982), The complete synthesis of seismic crustal phases at regional distances, *J. Geophys. Res.*, 87, 1735−1741.

Campillo, M., M. Bouchon, and B. Massinon (1984), Theoretical study of the excitation, spectral characteristics, and geometrical attenuation of regional seismic phases, *Bull. Seismol. Soc. Amer.*, 74, 79−90.

Cara, M., and J.B. Minster (1981), Multi-mode analysis of Rayleigh-type L_g, *Bull. Seismol. Soc. Amer.*, 71, 973−984.

Chouet, B. (1996), New methods and future trends in seismological volcano monitoring, in: *Monitoring and mitigation of volcano hazards*, ed. by R. Scarpa, and R.I. Tilling, pp. 23−97, Springer, Berlin.

Ewing, M., and A.P. Crary (1934), Propagation of elastic waves in ice, II, *Physics*, 5, 181−184.

Hagerty, M.T., M.A. Garces, S.Y. Schwartz, and M. Protti (1997), Long-term broad-band observations of ground deformations at Arenal Volcano, Costa Rica, *Eos, Trans. Amer. Geophys. Un.*, 78, (46), F431 [abstract].

Harris, I.McK., and P.G. Jollymore (1974), Iceberg furrow marks on the continental shelf Northeast of Belle Isle, Newfoundland, *Can. J. Earth Sci.*, 11, 443−524.

Knopoff, L. (1973), Interpretation of L_g, *Geophys. J. Roy. astr. Soc.*, 33, 387−402.

Kohnen, H. (1970), Über die Absorption elastischer longitudinaler Wellen im Eis, *Polarforschung*, 39, 269−275.

Langleben, M.P. (1969), Attenuation of sound in sea ice, 10−500 kHz, *J. Glaciology*, 8, 399−406.

Levitus, S, T.P. Boyer, J. Antonov, R. Burgett, and M.E. Conkright (1994), *World Ocean Atlas 1994*, NOAA/NESDIS, Silver Springs, Maryland.

Neave, K.G., and J.C. Savage (1970), Icequakes on the Athabasca glacier, *J. Geophys. Res.* 75, 1351−1362.

Okal, E.A., and J. Talandier (1997), *T* waves from the great 1994 Bolivian deep earthquake in relation to channeling of *S* wave energy up the slab, *J. Geophys. Res.*, 102, 27421-27437.

Okal, E.A., P.-J. Alasset, O. Hyvernaud, and F. Schindelé (2001), The deficient *T* waves of tsunami earthquakes, *Geophys. J. Intl.*, submitted.

Press, F., and M. Ewing (1951), Propagation of elastic waves in a floating ice sheet, *Trans. Amer. Geophys Un.*, 32, 673−678.

Qamar, A. (1988), Calving: A source of low-frequency seismic signals from Columbia Glacier, Alaska, *J. Geophys. Res.*, 93, 6615−6623.

Reymond, D., O. Hyvernaud, J. Talandier, and E.A. Okal (2001), *T* –wave detection of two underwater explosions off Hawaii on April 13, 2000, *Bull. Seismol. Soc. Amer.*, submitted.

Sinadinovski, C., K. Muirhead, S, Spiliopoulos, and D. Jespen (1999), Effective discrimination of icequakes on seismic records from Mawson station, *Phys. Earth Planet. Inter.*, 113, 203−211,

Smith, W.H.F., and D.T. Sandwell (1994), Bathymetric prediction from dense satellite altimetry and sparse shipboard bathymetry, *J. Geophys. Res.,* 99, 21803−21824.

Talandier, J., and E.A. Okal (1996), Monochromatic *T* waves from underwater volcanoes in the Pacific Ocean: Ringing witnesses to geyser processes?, *Bull. Seismol. Soc. Amer.,* 86, 1529-1544.

Thiel, E., and N.A. Ostenso (1961), Seismic studies on Antarctic ice shelves, *Geophysics*, 26, 706−715.

VanWormer, D., and E. Berg (1973), Seismic evidence for glacier motion, *J. Glaciology,* 12, 259−265.

Wysession, M.E., E.A. Okal, and K.L. Miller (1991), Intraplate seismicity of the Pacific Basin, 1913−1988, *Pure Appl. Geophys.,* 135, 261-359.

Table 1. Principal characteristics of the 13 events studied

Number	Date and time D M (J)	Epicenter (°S)	Epicenter (°E)	Duration (mn)	Peak-to-peak velocity at VAH (μm/s)	Remarks
1	15 AUG (228) 22:28:18.6	78.21	-168.61	1.3	1.23	Edge of Ross Ice Shelf. No data at RAR, RKT. Monochromatic signal (3.5 Hz) with overtones; sharp impulsive beginning.
2	08 NOV (313) 22:18:31.3	72.10	170.16	2	2.18	Borchgrevink Land. Relatively monochromatic; frequency fluctuates; no overtones.
3	12 NOV (317) 01:13:26.6	75.76	-175.75	8	0.62	Central Ross Sea. Generally weak at Antarctic stns. Narrow spectrum centered around 4 Hz. Strong final puff with frequency increasing with time.
4	12 NOV (317) 06:00 — 09:00	75.8	-175.8	3 hr	0.24	Central Ross Sea. Only traces in Polynesia (except VAH); No signal at SBA and Erebus. Long signal, generally monochromatic (2.5 to 4 Hz), with frequency fluctuations but few overtones.
5	14 NOV (319) 01:01:56.6	75.92	-175.60	3	0.81	Central Ross Sea. No data: Erebus; No signal: SBA. Relatively broad spectrum on acoustic records. Dominant frequency 2.5 Hz at VNDA.
6	19 NOV (324) ~ 02:30	75.8	-175.8	10	0.42	No signal: RSP except VAH. No data: Erebus, SBA. Broad spectrum (2 − 16 Hz). Assumed in same area as Events 3−5, based on times at VNDA & VAH.
7	21 NOV (326) 15:22	75.8	-175.8	10	0.24	No signal: Polynesia except VAH. No data: Erebus, SBA. Fluctuation of dominant *f*, leading to "snake-shaped" spectrogram. Assumed at same location as Events 4−6, based on VNDA & VAH times.
8	22 NOV (327) 21:32:13.0	75.85	-176.28	10	0.34	Central Ross Sea. No data: Erebus, SBA. Same general characteristics as Event 7.
9	05 DEC (340) 03:21:19.8	75.08	-177.75	8	0.30	Central Ross Sea. No data: Erebus; No signal: SBA. Broad spectrum (2 − 10 Hz), with dominant f = 2.9 Hz. Final sequence with sharply increasing frequency.
10	05 DEC (340) ~ 20:46	75.1	-177.8	15	0.32	Noisy record; broad spectrum (2 - 10 Hz), with 2 sequences; assumed to share location of Event 9.
11	15 DEC (350) 03:16:14	74.4	-178.4	10	0.44	Central Ross Sea. No signal: SBA. Broad spectra (2 - 12 Hz); weak correlation of acoustic and seismic records.
12	18 DEC (353) 09:56:29.1	74.82	-178.68	8	0.42	Central Ross Sea. Two parts; 1st short (30 s) with impulsive start; 2nd emergent and long (150 s). Broad spectrum.
13	14 JAN (014) 2001 17:36:10	67.0	141.5	7	1.31	Off Oates or George V Coasts. No signal: RKT; all Antarctic stations. Relatively broad spectrum with dominant *f* at 4, 5.5 and 7 Hz; first sequence ends abruptly, followed by short (60 s) puff, with spectrogram showing several lines of strongly decreasing frequencies (gliding). Location only tentative.

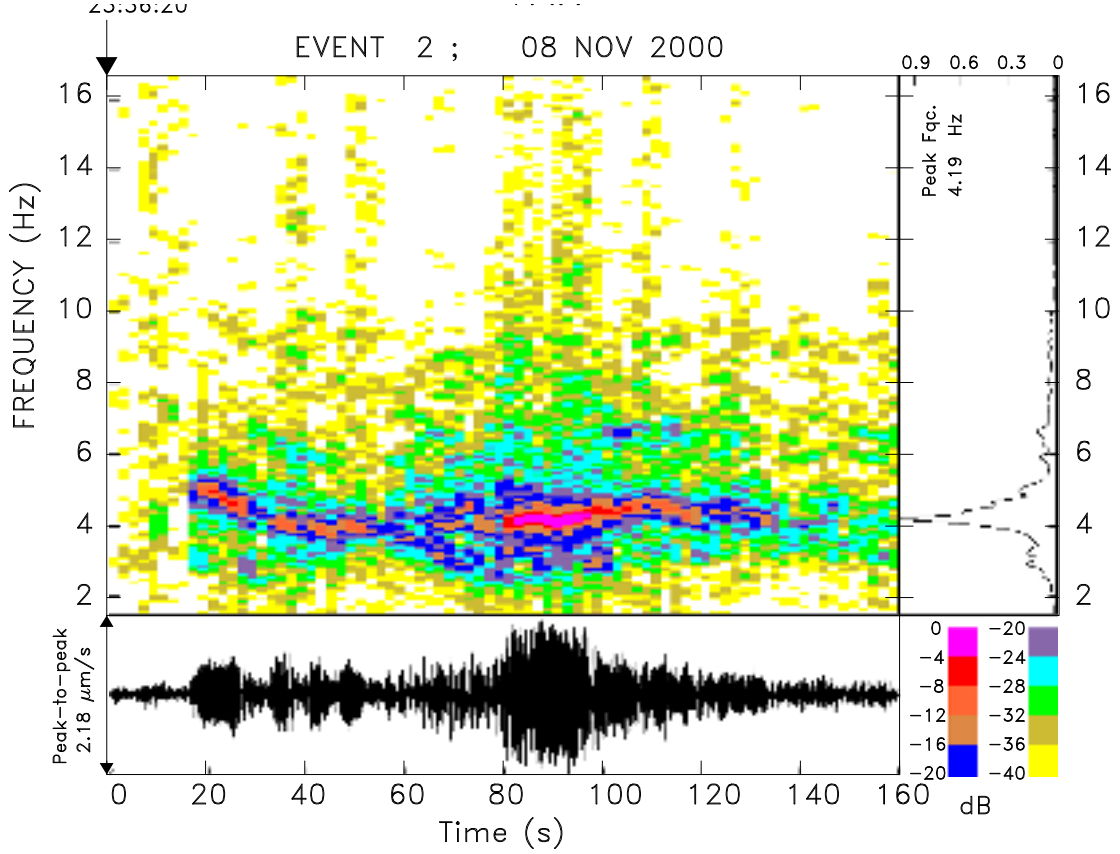

Figure 1a. T-phase record of Event 2 at Vaihoa. The figure is composed of three frames: The bottom one shows a 160-second time series of the ground velocity (in black), high-passed filtered for $f \geq 2$ Hz. The frame at right is a plot of the amplitude spectrum of the high-pass-filtered ground velocity record. The main color frame is a spectrogram representation of the distribution of spectral amplitude in the record, as a function of time and frequency. The color-coding is logarithmic, with the key (in dB relative to the most energetic pixel) given at bottom right. White pixels correspond to spectral amplitudes below −40 dB. Note the impulsive start of the signal, and the slow, contained, fluctuation of the prominent frequency with time.

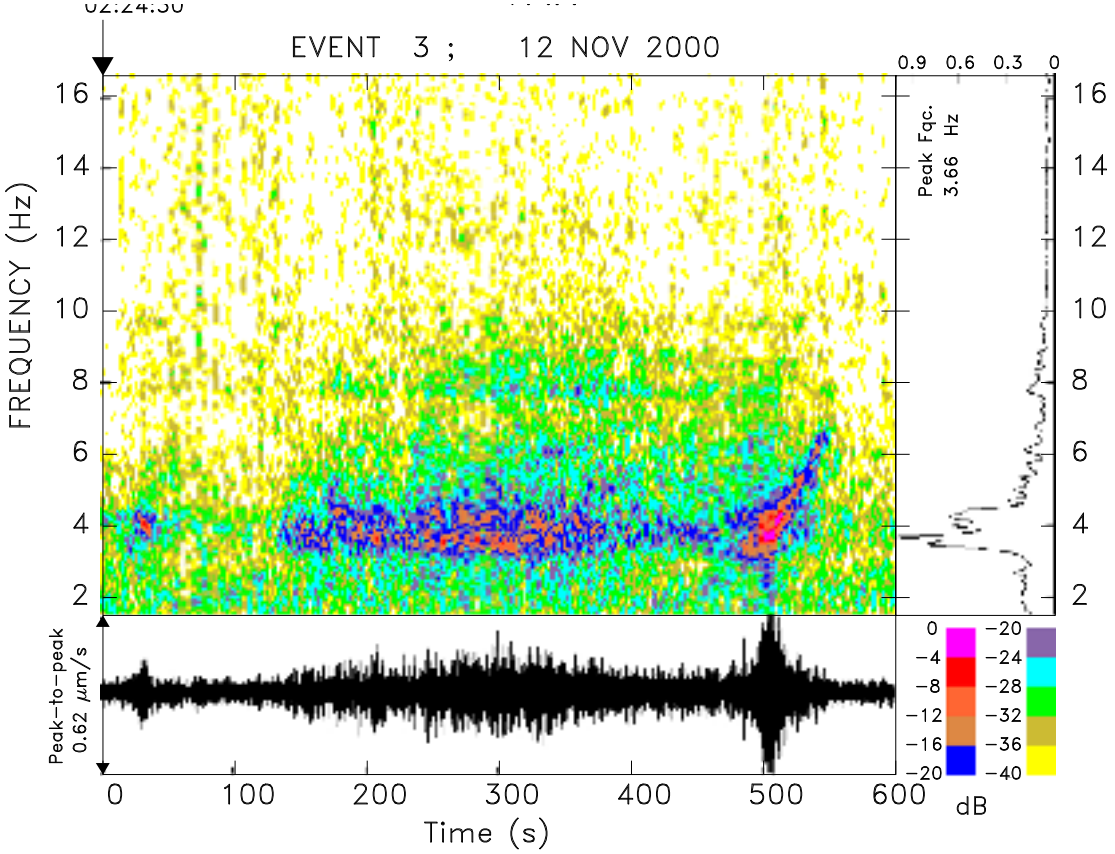

Figure 1b. Same as Figure 1a for Event 3. The time series is now 600−s long. Note the singular signal ending the sequence, featuring an increase of frequency with time.

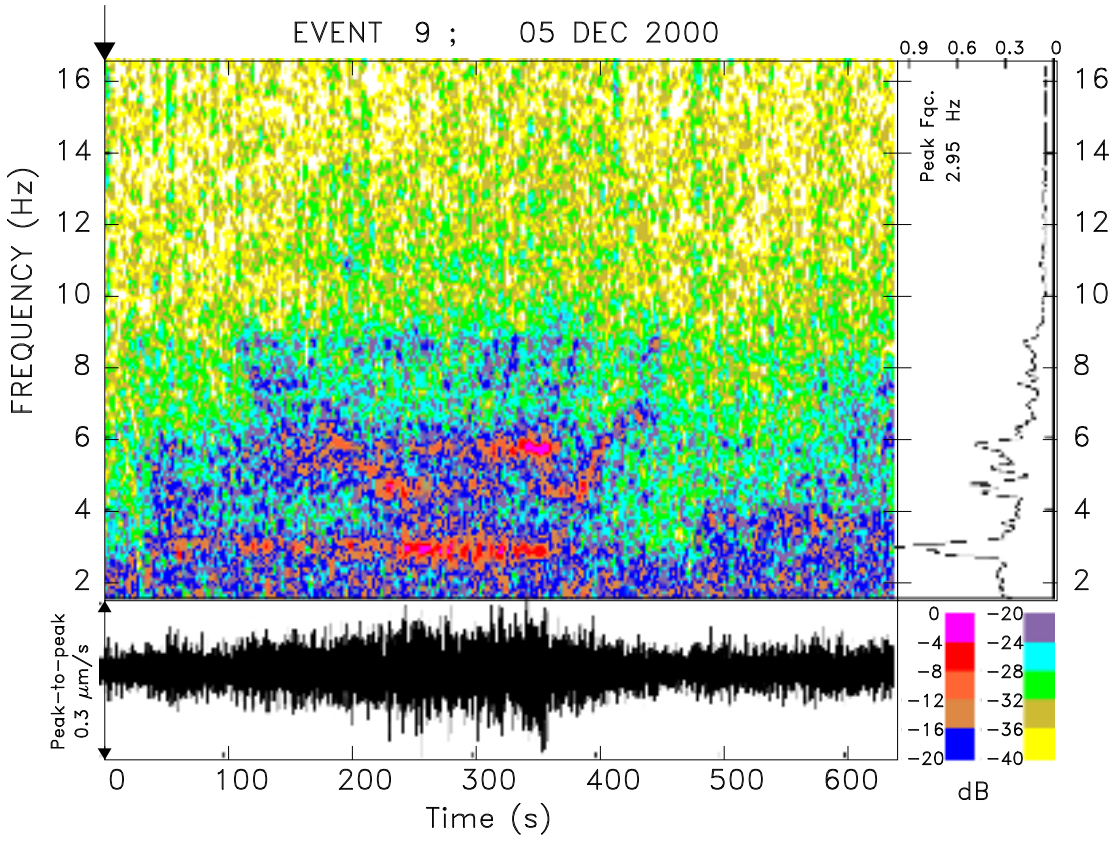

Figure 1c. Same as Figure 1a for Event 9. Note the relative complexity of the spectrum, and the trend towards an increase in frequency at the end of the main pulse (400 s into the signal).

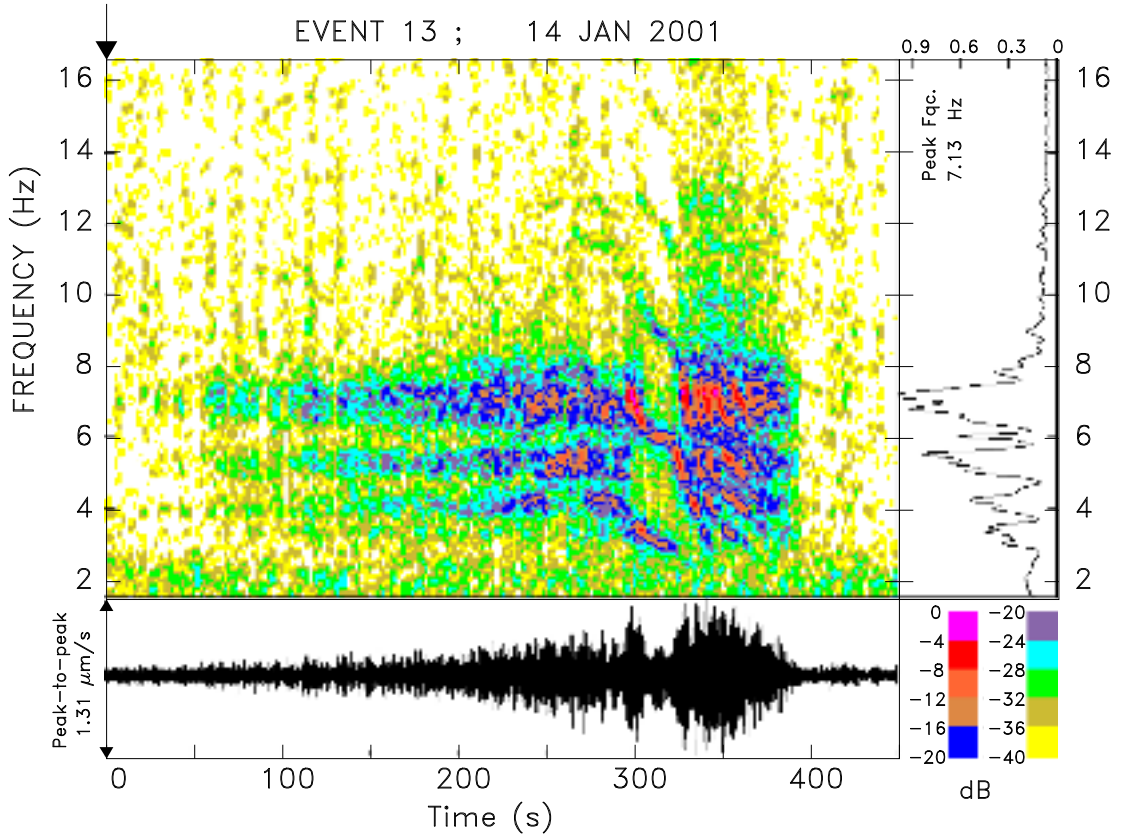

Figure 1d. Same as Figure 1a for Event 13. Note the complex character of the spectrogram, especially in the final phases of the pulse, where the eigenfrequency tends to decrease with time ("gliding").

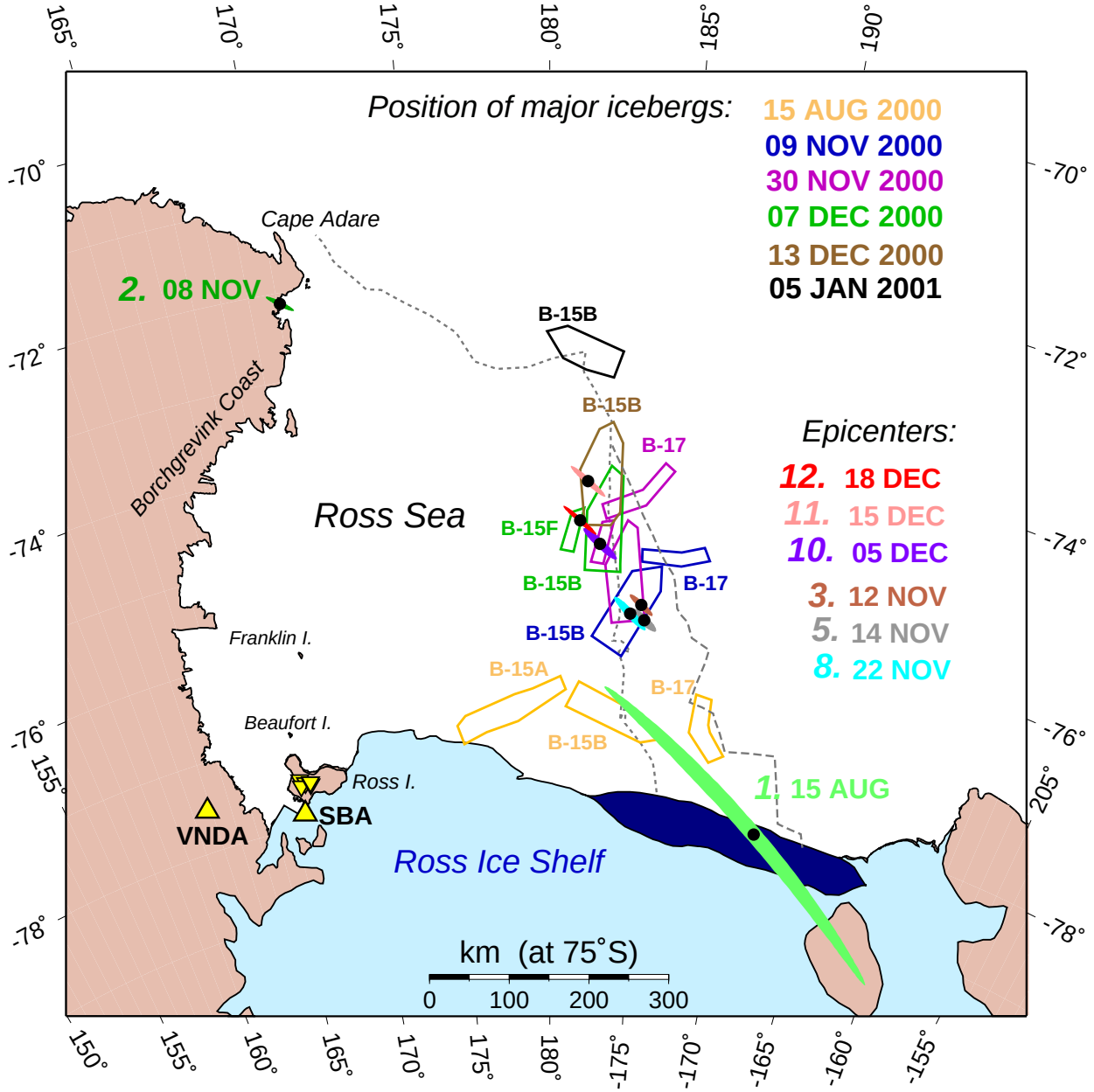

Figure 2. Final epicenters obtained by joint inversion of T-phase and seismic data. The individual epicenters are shown as black solid dots and the associated Monte Carlo ellipses are shaded (see color key at right; Event numbers in italics). The position of B-15 B is shown schematically at a number of dates from August 2000 to January 2001 (color-keyed; legend at top). Positions of the smaller iceberg B-17 are also shown at a few critical times until Late November 2000, when it breaks up into pieces following its collision with B-15 B. The paths of the two icebergs are also shown continuously by the dotted (B-15 B) and dashed (B-17) lines. The upward-pointing triangles show the global network seismic stations VNDA and SBA, the downward-pointing ones the MEVO network on Ross Island. The dark blue region schematizes the portion of the shelf which calved off and eventually gave rise to the B-15 and B-17 series. The projection is equidistant azimuthal centered at the South Pole.

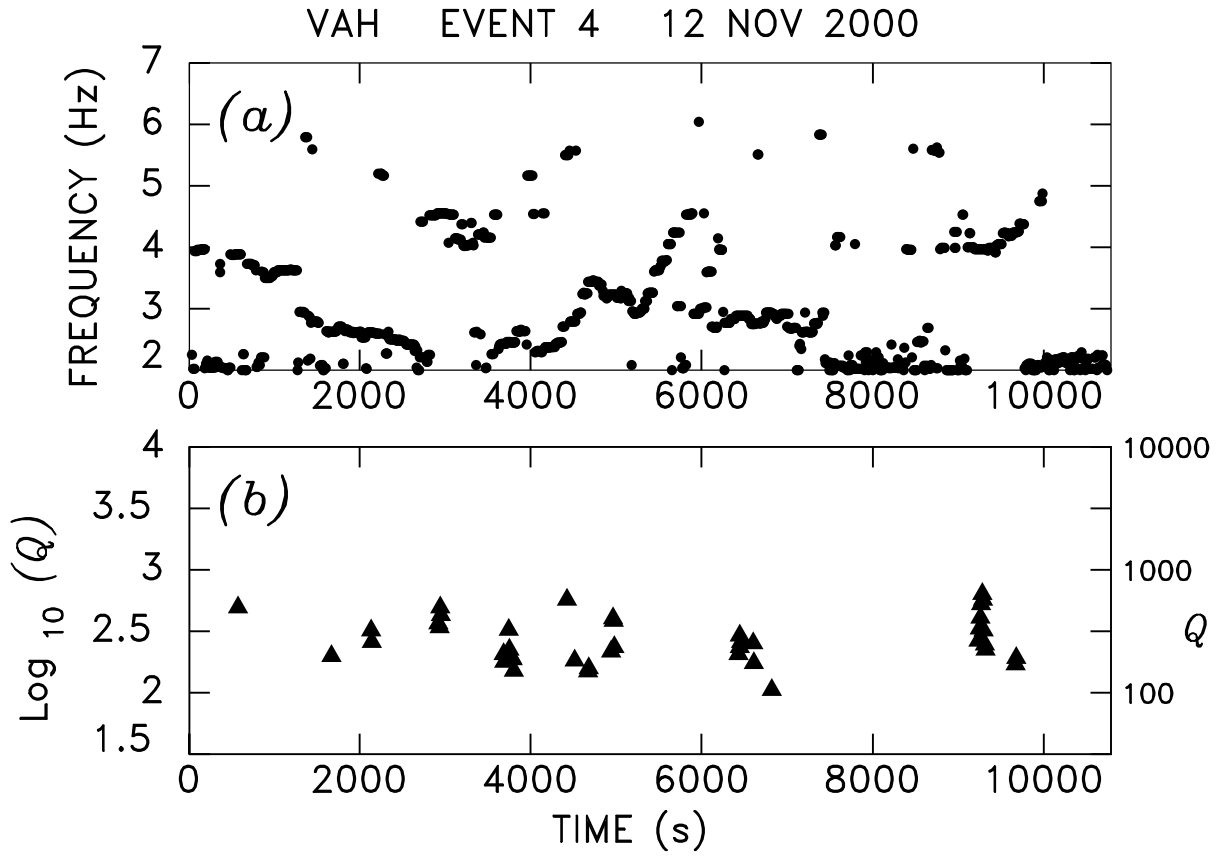

Figure 3. Evolution of spectral properties with time during Event 4. (a): Frequency f_0 at maximum of spectral amplitude. (b): Values of Q retained by application of quality thresholds.